A Hybrid RNN-based Deep Learning Model for Lung Cancer and COPD Detection

Raghuram Karla
Department of CSE, GST, GITAM, Visakhapatnam, India
rkarla@gitam.edu (corresponding author)

Radhika Yalavarthi
Department of CSE, GST, GITAM, Visakhapatnam, India
ryalavar@gitam.edu

Received: 19 June 2024 | Revised: 8 July 2024 | Accepted: 11July 2024

 DOI: https://doi.org/10.48084/etasr.8181

ABSTRACT

In the last ten years, lung cancer and chronic pulmonary diseases have become prominent respiratory diseases that require significant attention. This increase in prominence underscores their widespread impact on public health and the urgent need for better understanding, detection, and management strategies. Accurate identification of lung cancer and Chronic Obstructive Pulmonary Disease (COPD) is crucial for preserving human life. Accurate differentiation between the two disorders and the administration of the necessary treatment are very important. This study focuses on effectively discriminating between two of the deadliest chest diseases using chest X-ray images. Recurrent neural networks help to classify diseases accurately by improving feature extraction from radiographs. The proposed algorithm performs more effectively when analyzing chest X-ray image datasets showing alterations in a patient's chest, including the development of tiny lobes or thicker capillaries in the respiratory system among other details, compared to standard lung imaging.

Keywords-artificial intelligence; pulmonology; smoking; lobes; arterial infection

I. INTRODUCTION

Respiratory infections can have a wide range of symptoms, from minor self-limiting diseases, such as the common cold, influenza, and pharyngitis, to more serious conditions, such as lung cancer, severe acute respiratory syndromes, bacterial pneumonia, pulmonary embolism, tuberculosis, acute asthma, and Chronic Obstructive Pulmonary Disease (COPD). Recent global viral pandemics, such as COVID-19, are examples of respiratory diseases. Lung cancer develops in lung tissues, usually as a result of cells entering the airways. Small Cell Lung Cancer (SCLC) and Non-Small Cell Lung Cancer (NSCLC) are two main kinds. These classifications are based on how cells appear under a microscope. SCLC accounts for more than 80% of all cases. A progressive collection of lung disorders is known as COPD, with the most prevalent ones being chronic bronchitis and emphysema. Emphysema causes the lungs' air sacs to slightly shrink, obstructing external ventilation. The bronchial passages become inflamed and constricted due to bronchitis, allowing mucus to swell.

Smoking is the main cause of such a high incidence of diseases and fatalities [1]. About 85% of lung cancer incidences are related to heavy smoking. However, exposure to a smoking-friendly environment can also be a cause [2]. The ICMR has classified lung cancer as a slow pandemic in India. The annual death rate from these diseases demonstrates how crucial it is to diagnose them and receive the necessary care [3].

A wide variety of disorders that affect the lungs and impede their optimal functioning are referred to as lung diseases. Infections, environmental influences, genetic predispositions, and lifestyle decisions are among the numerous causes of these disorders. Coughing, dyspnea, thoracic distress, and reduced lung capacity are common symptoms of pulmonary disorders. The detection and diagnosis of lung disorders are essential for patient care, as they significantly impact health and quality of life. The global impact of pulmonary disorders is substantial. According to the World Health Organization (WHO), respiratory disorders, such as lung diseases, contribute substantially to global mortality. In 2016, respiratory disorders were the fourth most common cause of mortality worldwide, contributing to approximately 3.0 million deaths. This elevated mortality rate is influenced by conditions such as lung cancer, COPD, and pneumonia. The impact of lung disorders on public health is significantly reduced by prompt identification and precise diagnosis.

Many studies focus on how artificial neural networks help improve the classification and prediction of such diseases. This study deploys ResNet18 to classify images into various subcategories. Artificial Intelligence (AI) uses computers and technology to replicate intelligent behavior and critical thinking

comparable to humans. In addition, it allows individuals to assess and understand intricate medical information, helping to diagnose, manage, and predict treatment outcomes in various clinical scenarios. AI can revolutionize the medical sector. With its newest breakthroughs, AI applications have grown into sectors that were previously thought to be unattainable without human experience due to the availability of digital data, machine learning, and computer infrastructure. In recent years, Deep Learning (DL) has made significant advances in the fields of caption generation, image identification, and speech recognition.

A. Challenges in Lung Cancer Detection

- Radiographic Variability: Lung cancer can manifest in diverse radiographic forms, such as small nodules, masses, and infiltrates. These can pose difficulties in distinguishing them from non-cancerous conditions, such as infections, fibrosis, or other lung diseases.
- Subtle Lesions: In the early stages, lung cancer can appear as inconspicuous abnormalities that can go unnoticed, particularly when there are overlapping anatomical components, such as the ribs, blood arteries, and the heart.

B. Benefits of Employing Deep Learning (DL)

DL methods offer numerous benefits compared to conventional ones.

- Automated Feature Extraction: DL models can autonomously acquire and extract pertinent features from unprocessed images, eliminating the need for manual feature engineering. This is especially advantageous in medical imaging, as it can be difficult to precisely identify complicated patterns and subtle features.
- DL models can obtain a notable level of precision and reliability in identifying lung cancer by acquiring knowledge from extensive collections of annotated images. They are capable of delivering consistent results and minimizing variations between different readers.
- Convolutional Neural Networks (CNNs) can identify complicated patterns and spatial structures within images, making them highly effective in detecting subtle and diversified signs of lung cancer.
- Scalability: After training, DL models can rapidly process substantial amounts of images, making it easier to implement large-scale screening programs and reducing the amount of labor required for radiologists.

II. LITERATURE STUDY

Many studies have used different approaches and DL models to process images and detect cancer. DL is a widely recognized method to investigate the application of multiview image registration and fusion techniques in the detection of lung cancer. In [4], it was shown that combining multiple imaging views can significantly improve the detection accuracy of malignant lesions. This approach took advantage of the strengths of different imaging modalities, such as CT and X-ray images, to provide a comprehensive view of lung tissues and facilitate more precise identification of cancerous regions. In [5], the focus was on improving the prediction and classification accuracy of lung cancer and chronic obstructive pulmonary disorders. In [6], early identification of cancer nodules in the lungs was performed utilizing Computer-Aided Detection (CAD) systems using Low Dose Computed Tomography (LDCT) images. This study underscored the importance of employing various DL models on raw data. In [7], Deep CNNs were used to analyze chest X-ray images for COPD identification, showing superior performance compared to traditional methods.

In [8, 9], radiomics and gene expression profiles were employed along with DL algorithms to characterize diseases and predict outcomes in patients with lung cancer. In [10], a hybrid DL model was proposed to detect and classify lung cancer from fusion images utilizing MCNet. This study contributed to the advancement of the field of medical imaging by integrating multiple modalities and leveraging DL techniques to enhance diagnostic accuracy and efficacy in oncological diagnostics. In [11], chest X-ray images and DL approaches were deployed to diagnose lung-related diseases. The ChesXNet can help a radiologist diagnose pneumonia. In [12], the Libre Health Radiological Information System (RIS) was developed using an open-source alternative to Electronic Health Record (EHR) systems. This system achieved a good accuracy rate in correctly identifying diseases. In [13], data augmentation methods were applied to address several issues with medical images and validate and enhance the accuracy of the CNN model.

In [14, 15] small nodules were detected using probabilistic neural networks and bioinspired reinforcement learning. Pre-set neural network groups were integrated following the fuzzy logic method. These techniques were combined to identify tiny lung nodules linked to lung cancer. The type-1 fuzzy approach was adopted to analyze a series of X-ray images as input, and then the neural network was used to provide the final judgment. In [16], CT scans were implemented for rapid segmentation of lung segments, using a Progressive Dense V-Network and a 3D CNN. This system achieved segmentation of small lung lobes in approximately 2 seconds per forward pass. The approach proposed in [17] facilitated a swift and reliable diagnosis of diverse lung diseases, encompassing prevalent conditions such as COPD and lung cancer. This study incorporated healthy and diseased lung CT images. In [18], CNNs and Transfer Learning (TL) techniques were deployed to identify different chest diseases. DL was utilized to facilitate the connection between basic and complex information. As imaging technology generates fundamental data, human expertise adds nuanced understanding. To streamline the process, a pre-existing model was fine-tuned, rather than creating a new CNN model from the ground up, to address an ongoing challenge in medical imaging research.

In [19, 20], the DeTrac technique was used within a CNN architecture, incorporating the disintegration, deportation, and composition methods (DeTrac). This approach focused on class disintegration, using TL to enhance the effectiveness of classifying medical images. Various image types, including digital mammograms, colon cancer histological images, and chest radiographs, were processed utilizing this technique. In

[21], data mining and supervised learning techniques were employed to classify lung carcinomas on multi-dimensional datasets. Based on the image sets collected, the algorithm determines whether the patient had or has a probability of developing lung carcinoma. The scan analysis was classified as malignant if even one node was determined to be diseased. This approach focused on enhancing traditional early detection techniques for lung carcinomas. In [22], MobileNet was used to classify lung diseases from chest radiographs. This system goes through each batch of images to find aberrant areas that are different from the typical set of images. Adam optimizer was deployed to analyze loss values, perform backpropagation, and optimize the selection of hyperparameters and trainable parameters. This approach demonstrated the effectiveness of deep networks in providing highly accurate classification and predictive capabilities. In [23, 24], lung carcinomas were identified using an artificial neural network and a support vector network. These algorithms were applied to evaluate their performance and determine which can provide a better prediction. Several criteria were used to assess the classifiers' effectiveness. In [25], machine learning methods were applied to detect and diagnose COPD and asthma. The primary goal was to determine whether machine learning algorithms could make predictions and perform variable importance evaluation.

III. MATERIALS AND METHODS

A. Dataset

The Lung X-Ray Image dataset [26] is a comprehensive collection of X-ray images that is essential for the identification and diagnosis of lung disorders. The dataset comprises 3,475 X-ray images that are classified into three distinct categories:

- Standard (1250 images): These images illustrate typical lung conditions and are used as a reference during diagnostic procedures.
- Lung Opacity (1125 images): This category contains X-ray images that exhibit a variety of lung irregularities, showing a variety of cases for investigation.
- Viral Pneumonia (1100 images): These images are associated with cases of viral pneumonia, thus facilitating the identification of this specific respiratory condition.

The Lung X-Ray Image dataset is of the utmost importance to the healthcare industry, as it provides a comprehensive and well-documented collection of X-ray images. These images are essential for the identification, categorization, and understanding of respiratory disorders. This resource is substantial for the improvement of patient outcomes and the advancement of the field of respiratory medicine.

B. Dataset Preprocessing

All images were downsized to 100×100 pixels to improve feature extraction. The deletion, selection, and partitioning stages of the features were simplified by this step [3]. Grayscale images were converted to RGB to enhance the characterization of evidently distinct disease-affected nodules, facilitating predictive analysis. Before moving to the initial layer, the images were subjected to max pooling and stride functions. Stride was employed to shift pixels within a frame, the stride ratio was chosen as 2, and pooling aimed to collect the image's most important details. A kernel was used to extract features. This is a kind of filter to strip features from captured images. Its primary function is to help in the extraction of higher-level characteristics from the margins of pictures that are occasionally overlooked, resulting in a feature map. The feature map contains all the features taken from the image set. Until it reaches the fully connected layer, it serves as an input for the next layer in the system. The feature map differs depending on the channel. For example, the grayscale feature map has a 3×3 filter, 3×3×1 for every block, and the RGB feature map has a 3×3 filter, 3×3×3 for every block.

C. Data Augmentation

Data augmentation was used to increase the neural network training dataset. Contrast adjustment and Gaussian blur are indispensable for training neural networks for medical image interpretation. The network can identify and distinguish regions of interest as a result of enhanced feature differences that are facilitated by image contrast. This enables the network to effectively manage fluctuations in clinical illumination. Gaussian blur reduces high-frequency noise, which can lead to overfitting, and improves generalization, enabling the network to identify features in images that are indistinct or have been preprocessed. The contrast of each image was improved to generate augmented images employing a linear algorithm. Gaussian blur was utilized to achieve a subtle blur without flattening.

Horizontal rotation was used to enhance the resilience of the neural network. Horizontal flipping is a fundamental data augmentation technique that enhances neural networks by introducing symmetry and variation into the training sample. The network acquires the ability to identify and differentiate properties despite their side orientation by reflecting images across the vertical axis. This serves to mitigate unilateral body deformities. In medical imaging, diagnostic reliability is enhanced by reflected anomalies, which are essential for accurate identification and division of characteristics in a variety of patient scenarios and imaging views. The same augmentation techniques were employed to generate a new set of blurred and contrasted images after they were flipped horizontally. The dataset was expanded by these augmentations, which also included a diverse array of imaging-related modifications. Various data are required for a neural network to accurately identify and separate lung sections in chest X-ray images under a variety of circumstances.

The Adam optimizer was deployed to optimize the model, which was trained using a cross-entropy loss function. The learning rate was meticulously calibrated to ensure efficient convergence. Validation loss and accuracy were monitored during the training process to identify overfitting and modify the hyperparameters as necessary.

D. Hybrid Recurrent Neural Network (RNN)

The proposed hybrid model utilizes a ResNet18 architecture as the backbone for feature extraction. While the core structure of ResNet18 remained intact, several key modifications were introduced to enhance its suitability for detecting lung cancer and COPD in chest X-ray images.

1) Input Layer Adjustments

The original ResNet18 is designed to handle RGB images with a size of 224×224 pixels. However, the dataset consists of grayscale chest X-ray images resized to 100×100 pixels. Therefore, the input layer was adjusted to accept these dimensions, converting grayscale images to three-channel inputs by duplicating the single channel across the RGB channels to maintain compatibility with the pre-trained weights.

2) Feature Extraction Layers

The 18-layer architecture of ResNet18 includes convolutional layers, batch normalization, ReLU activations, and max-pooling layers. These layers are crucial to extract hierarchical features from the input images.

3) Incorporation of RNN

An RNN layer was used to capture temporal dependencies and sequential patterns in the image data after the feature extraction stage, as shown in Figure 1. This hybrid approach leverages the strengths of both CNNs for spatial feature extraction and RNNs for handling sequential data. Specifically, a Long Short-Term Memory (LSTM) layer was employed, which processes the sequential features generated by the ResNet18 layers.

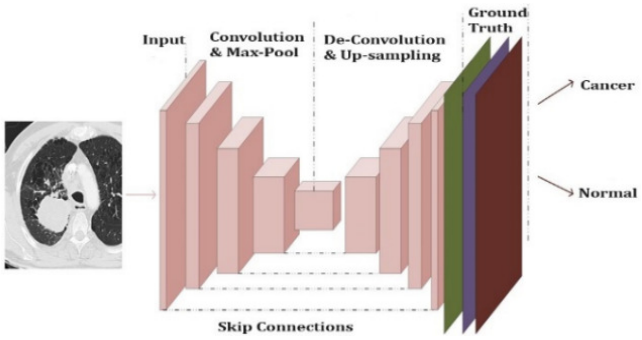

Fig. 1. RNN architectural framework.

4) Fully Connected Layer

The final layer of ResNet18 was replaced with a custom fully connected layer tailored to this classification task. This layer outputs predictions for the specific classes related to lung cancer and COPD. These modifications are justified in the results section as they blend the traditional convolutional approach with RNN capabilities, enhancing the model's performance on this specialized task.

E. Deep Learning Techniques

DL is one of the rapidly growing subfields within machine learning. In CNNs applied to medical imaging, multiple layers often act as spatial filters that seamlessly integrate different levels of information. For instance, even when the input data are not specifically segregated into pulmonary fields, these layers effectively process the input collection [15]. The CNN architecture has a wide range of parameters or components to help identify the impacted nodules. Its exceptional performance in several challenging domains, such as biomedical imaging applications, including imaging diagnostics, isolation, and separation, has attracted increased interest from researchers in recent years [27]. The features of an image are usually composed of pixels arranged in a matrix. To avoid underfitting, learning should be performed using a sizable number of data pictures before modifying the CNN settings. The extracted deep feature vector has demonstrated a remarkable ability to precisely characterize training data and effectively discern between normal, malignant, and lung nodules.

The decision to integrate RNN layers with ResNet18 stems from the nature of medical image data and the specific requirements of the objective. Lung X-rays can exhibit subtle temporal changes that are crucial for accurate diagnosis. By incorporating RNNs, the proposed model can better capture these temporal patterns and dependencies, leading to more robust and accurate classifications. The combination of CNN and RNN architectures enables the model to leverage spatial and sequential features, providing a comprehensive analysis of chest X-ray images.

F. Linear Discriminant Analysis (LDA)

The linear discrimination algorithm is one of the techniques employed in the preprocessing phase of machine learning and pattern detection to reduce dimensionality. This algorithm is used to reduce the specificity of the dimension space, thus preventing excessive matching and reducing computational costs. It is comparable to Principal Component Analysis (PCA), which is employed to increase the data variability and optimize the distinction between various classes found in picture sets. LDA, as given in (1), preserves class discriminating data in the shortest subspace k, where $k = n$-1. By limiting estimates of parameters, dimensionality reduction not only reduces system processing costs for classification but also helps in preventing overmatching.

$$log\left(\frac{\frac{1}{\sqrt{2\Pi}\sigma}\ell^{\frac{-1}{2}\left(\frac{X-\mu_i}{\sigma}\right)^2}P(Y=i)}{P(X=a)}\right) \quad (1)$$

$$= log\left(\frac{1}{\sqrt{2\Pi}\sigma}\ell^{\frac{-1}{2}\left(\frac{X-\mu_i}{\sigma}\right)^2}\right) + log\big(P(Y=i)\big) - log\,P\,(X=a)$$

$$= log\left(\frac{1}{\sqrt{2\Pi}\sigma}\right) - \frac{1}{2}\left(\frac{X-\mu_i}{\sigma}\right)^2 + log\big(P(Y=i)\big)\; - log\,P\,(X=a)$$

$$= log\left(\frac{1}{\sqrt{2\Pi}\sigma}\right) - \frac{1}{2}\frac{X^2}{\sigma^2} + \frac{\mu_i X}{\sigma^2} - \frac{1}{2}\frac{{\mu_i}^2}{\sigma^2} + log\big(P(Y=i)\big) - log\,P\,(X=a)$$

$$\boldsymbol{\delta}(X) = \frac{\boldsymbol{\mu_i^2 X}}{\boldsymbol{\sigma^2}} - \frac{\mathbf{1}}{\mathbf{2}}\frac{\boldsymbol{\mu_i^2}}{\boldsymbol{\sigma^2}} + log\big(P(Y=\boldsymbol{i})\big)$$

The following are the steps utilized to implement LDA:

- For every class in the data, a d-dimension mean vector is calculated.
- Scattering matrices are calculated both within and across classes.
- Eigenvectors and associated eigenvalues are calculated.
- Based on eigenvalues, eigenvectors are arranged in a decreasing order.
- The eigenvalues have a d×k shape.

- Unique subspaces are transformed using *d*×*k*, resulting in Y=X×W.

G. Feature Extraction

The ResNet18 model begins with the convo1 block, integrating convolutional operations, batch normalization, and max pooling algorithms. Convolutions involve applying a kernel across an image or input volume, facilitating feature extraction and spatial information processing. Matrix multiplication is performed when the image's value and kernel's size fit. The outcome of this value goes to the next layer. The feature map is 64 pixels in size, whereas the kernel size is assumed to be 7. For many ResNet topologies, this number varies. The result size of convol1 is 112×112. The subsequent action is batch normalization, which is employed to perform actions on elements without altering the volume size. Max pooling is used to get the highest value from the supplied collection of matrices.

Following the preprocessing phase, the images are included in the system. Resnet18 is organized into four levels, each of which has a set number of sublayers. The kernel size in layer 1 is (33, 64), which is different from the convo1 block. The volume size does not vary within the block, even if the values for two kernels vary. This is because these layers have their maximum pooling and stride settings applied. This block's output size is 56×56. In this step, equations (1) and (2) are applied to the image. Figure 4 depicts the architectural outline.

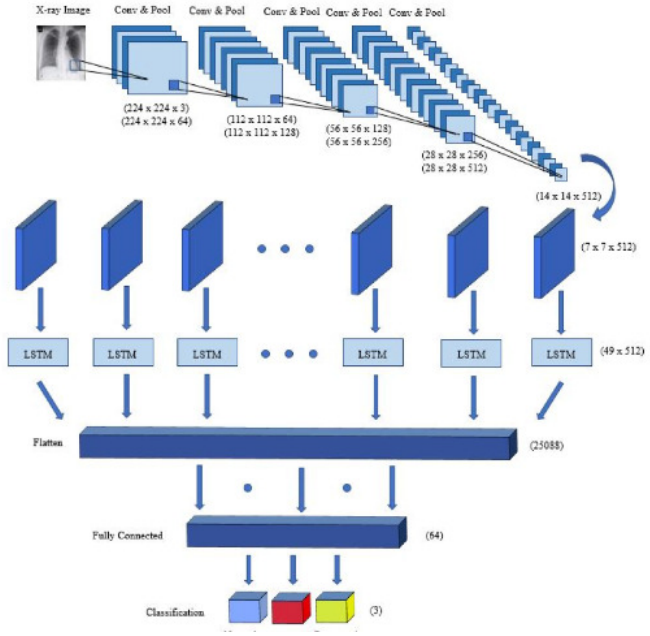

Fig. 2. The proposed hybrid method for lung cancer detection.

$$Output = \frac{Input-N+2R}{M} \quad (2)$$

Every layer's input and output dimensions vary. For example, the system's beginning dimensions are 100 by 100 and its ultimate result is 1 by 1. Following the use of mean pooling, this provides the final expected outcome. The kernel size of the second layer is (33, 128), and it receives input from the layer above it. The skipping connection is shown as a dot layer. Every layer goes through a decrease in size during its initial step. The skipping layers are employed to resize this dimensionality as in (3).

$$\vec{act}[m] = W_{x_u}\vec{x}[n] + W_{s_u}\vec{S}[k-1] + W_{v_{cu}}\vec{v}[k-1] + b\vec{a}S_u$$

$$\vec{act_s}[m] = W_{x_{cs}}\vec{x}[n] + W_{s_{cs}}\vec{S}[n-1] + W_{v_s}\vec{v}[k-1] + \vec{b}_{cs}$$

$$\vec{act_r}[n] = W_{x_r}\vec{x}[n] + W_{s_r}\vec{S}[n] + W_{v_r}\vec{v}[n-1] + \vec{b}_{cr}$$

$$\vec{act_u}[n] = W_{x_u}\vec{x}[n] + W_{v_u}\vec{v}[n-1] + \vec{b}_u$$

$$\vec{u}[n] = G_d\left(\vec{act_u}[n]\right) \quad (3)$$

IV. EXPERIMENTS AND RESULTS

The proposed technique was tested and evaluated according to accuracy, duration, validation loss, learning loss, wall time, and disease prediction performance. Jupyter Labs was deployed to develop the system. The system was first trained using a particular collection of images (training set), after which predictions on the test set were made. Labeled (green) and unlabeled (red) data were present in the image sets. The system was trained over 20 epochs during which it classified images and displayed validation loss and prediction accuracy. The initial validation loss and accuracy for the first epoch were 0.3517 and 0.787, respectively. At the end of the training process, the validation loss decreased to 0.0383, while the accuracy increased to 0.962. This improvement indicates that the model effectively learned from the training data and made more accurate predictions. However, it is essential to monitor for overfitting, where the model may perform well on the training data but struggle with new data, which would be indicated by increasing validation loss and accuracy scores.

Table II illustrates the effectiveness and defect rates of several classifications. Although most classifiers work at a rate of greater than 80%, a growth in error rates decreases their ability to classify diseases while also decreasing the effectiveness of the entire system.

TABLE I. COMPARATIVE PERFORMANCE OF THE PROPOSED WITH EXISTING MODELS [28, 29]

Classifiers	Accuracy	Error rate
AlexNet	94.32%	12.30%
VGG16	92.45%	8.70%
GoogleNet	95.32%	5.32%
ResNet	95.89%	2.17%
SVM	95%	3.51%
CheXNet	88%	4%
CNN	89%	15.87%
Hybrid RNN	96.2%	3.8%

V. DISCUSSION

The RNN is crucial for accurate prediction of diseases from X-ray images. The proposed system divides the pictures into

several layers and then performs feature extraction, which yields the final result of image processing and disease detection. Other studies used various DL techniques for the same objective. Most of the approaches had a variety of flaws that resulted in lower performance. The proposed method employed a single dataset for training and testing. Class disparity is a common issue in machine learning, being the result of various classes having different sample sizes [6]. This is because there are more negative samples than positive ones. The proposed system avoided the disappearing gradient problem that most of the previously suggested systems had. This is a major concern, since the system eventually stopped learning new features. In simpler terms, it is about shrinking dimensions by minimizing differences within groups and maximizing gaps between groups. Enhancing the distance between two distinct classes ameliorates the system's ability to delineate boundaries, thereby refining classification outcomes. The system leveraged image datasets to aid in disease detection, employing diverse methods to maximize information extraction. Each procedural step prioritized the acquisition of highly discriminative features, thereby boosting the system's accuracy in classifying images. Although there are alternative algorithms, such as PCA, evaluations favored LDA for its superior feature-handling capabilities.

TABLE II. MODEL SPECIFICITY AND SENSITIVITY [28-29]

Classifiers	Specificity	Sensitivity
VGG19, SVM	92.41%	93%
MultiLayerPerceptron	52.45%	65.41%
CheXNet	NA	82.1%
ANN	89.01%	93.25%
CNN	NA	NA
ML	93.10%	95.61%
Probabilistic neural network	NA	NA
Residual neural network	92.07%	92.71%
Support Vector Machine	91.15%	92%
Progressive dense V-N/w	83.10%	NA
VGG16	94.00%	NA
MobileNet	84%	81.2%
Hybrid RNN (proposed model)	96.02%	96%

VI. INFERENCES

Many errors were discovered in many studies using diverse methods. In certain instances, the algorithms misclassified many diseases. Poor performance is the result of a system's inability to effectively extract the features from images and train them/be trained to recognize the conditions. The TL approach also presents issues. A system must be trained to work on new features and be able to independently solve new issues using the knowledge it gains from solving older ones. On rare occasions, though, it failed, and fresh ones had to be produced by training the system. Data privacy was one of the main issues raised in some studies. Patient records, which held all of the user's data, had to be appropriately maintained for the detection of diseases, but there was no assurance for this. Occasionally, the system was unable to maintain the privacy of these data. The computational cost is still another significant downside.

VII. CONCLUSION

The proposed hybrid system efficiently analyzes X-ray images to classify them as lung cancer, normal, and COPD. Based on the ResNet18 algorithm, each additional technique was employed to process the images into matrices and ensure accurate classification. The key to its performance is feature extraction, crucial to improving prediction accuracy, achieved through various operations such as stride, max pooling, and average pooling across layers to maintain dimensionality. The system focuses on training the model using extracted features to facilitate the learning and prediction of the targeted diseases. Its predictive ability can help in the detection and diagnosis of lung cancer and COPD. Therefore, the system has immense potential to advance medical practice and potentially save lives. Future endeavors could expand this method to anticipate other visually diagnosable diseases.

REFERENCES

[1] D. Moitra and R. Kr. Mandal, "Automated AJCC (7th edition) staging of non-small cell lung cancer (NSCLC) using deep convolutional neural network (CNN) and recurrent neural network (RNN)," *Health Information Science and Systems*, vol. 7, no. 1, Jul. 2019, Art. no. 14, https://doi.org/10.1007/s13755-019-0077-1.

[2] C. Tejaswini, P. Nagabushanam, P. Rajasegaran, P. R. Johnson, and S. Radha, "CNN Architecture for Lung Cancer Detection," in *2022 IEEE 11th International Conference on Communication Systems and Network Technologies (CSNT)*, Indore, India, Apr. 2022, pp. 346–350, https://doi.org/10.1109/CSNT54456.2022.9787650.

[3] A. Asuntha and A. Srinivasan, "Deep learning for lung Cancer detection and classification," *Multimedia Tools and Applications*, vol. 79, no. 11, pp. 7731–7762, Mar. 2020, https://doi.org/10.1007/s11042-019-08394-3.

[4] I. Nazir, I. ul Haq, S. A. AlQahtani, M. M. Jadoon, and M. Dahshan, "Machine Learning-Based Lung Cancer Detection Using Multiview Image Registration and Fusion," *Journal of Sensors*, vol. 2023, no. 1, 2023, Art. no. 6683438, https://doi.org/10.1155/2023/6683438.

[5] J. J. Chabon *et al.*, "Integrating genomic features for non-invasive early lung cancer detection," *Nature*, vol. 580, no. 7802, pp. 245–251, Apr. 2020, https://doi.org/10.1038/s41586-020-2140-0.

[6] P. R. Radhika, R. A.S. Nair, and G. Veena, "A Comparative Study of Lung Cancer Detection using Machine Learning Algorithms," in *2019 IEEE International Conference on Electrical, Computer and Communication Technologies (ICECCT)*, Coimbatore, India, Feb. 2019, pp. 1–4, https://doi.org/10.1109/ICECCT.2019.8869001.

[7] M. A. Heuvelmans *et al.*, "Lung cancer prediction by Deep Learning to identify benign lung nodules," *Lung Cancer*, vol. 154, pp. 1–4, Apr. 2021, https://doi.org/10.1016/j.lungcan.2021.01.027.

[8] M. Kirienko *et al.*, "Radiomics and gene expression profile to characterise the disease and predict outcome in patients with lung cancer," *European Journal of Nuclear Medicine and Molecular Imaging*, vol. 48, no. 11, pp. 3643–3655, Oct. 2021, https://doi.org/10.1007/s00259-021-05371-7.

[9] D. Mhaske, K. Rajeswari, and R. Tekade, "Deep Learning Algorithm for Classification and Prediction of Lung Cancer using CT Scan Images," in *2019 5th International Conference On Computing, Communication, Control And Automation (ICCUBEA)*, Pune, India, Sep. 2019, pp. 1–5, https://doi.org/10.1109/ICCUBEA47591.2019.9128479.

[10] B. L. Nandipati and N. Devarakonda, "Hybrid deep learning model for detection and classification of lung cancer fusion images using MCNet," *Journal of Intelligent & Fuzzy Systems*, vol. 45, no. 2, pp. 2235–2252, Jan. 2023, https://doi.org/10.3233/JIFS-231145.

[11] G. M. Agazzi *et al.*, "CT texture analysis for prediction of EGFR mutational status and ALK rearrangement in patients with non-small cell lung cancer," *La radiologia medica*, vol. 126, no. 6, pp. 786–794, Jun. 2021, https://doi.org/10.1007/s11547-020-01323-7.

[12] K. E. Mullins, C. Seneviratne, A. C. Shetty, F. Jiang, R. Christenson, and S. Stass, "Proof of concept: Detection of cell free RNA from EDTA plasma in patients with lung cancer and non-cancer patients," *Clinical Biochemistry*, vol. 118, Aug. 2023, Art. no. 110583, https://doi.org/10.1016/j.clinbiochem.2023.05.002.

[13] W. Wang and G. Charkborty, "Automatic prognosis of lung cancer using heterogeneous deep learning models for nodule detection and eliciting its morphological features," *Applied Intelligence*, vol. 51, no. 4, pp. 2471–2484, Apr. 2021, https://doi.org/10.1007/s10489-020-01990-z.

[14] G. Capizzi, G. L. Sciuto, C. Napoli, D. Połap, and M. Woźniak, "Small Lung Nodules Detection Based on Fuzzy-Logic and Probabilistic Neural Network With Bioinspired Reinforcement Learning," *IEEE Transactions on Fuzzy Systems*, vol. 28, no. 6, pp. 1178–1189, Jun. 2020, https://doi.org/10.1109/TFUZZ.2019.2952831.

[15] N. Cherukuri, N. R. Bethapudi, V. S. K. Thotakura, P. Chitturi, C. Z. Basha, and R. M. Mummidi, "Deep Learning for Lung Cancer Prediction using NSCLS patients CT Information," in *2021 International Conference on Artificial Intelligence and Smart Systems (ICAIS)*, Coimbatore, India, Mar. 2021, pp. 325–330, https://doi.org/10.1109/ICAIS50930.2021.9395934.

[16] S. K. Thakur, D. P. Singh, and J. Choudhary, "Lung cancer identification: a review on detection and classification," *Cancer and Metastasis Reviews*, vol. 39, no. 3, pp. 989–998, Sep. 2020, https://doi.org/10.1007/s10555-020-09901-x.

[17] C. L. Chen *et al.*, "An annotation-free whole-slide training approach to pathological classification of lung cancer types using deep learning," *Nature Communications*, vol. 12, no. 1, Feb. 2021, Art. no. 1193, https://doi.org/10.1038/s41467-021-21467-y.

[18] P. M. Shakeel, M. A. Burhanuddin, and M. I. Desa, "Automatic lung cancer detection from CT image using improved deep neural network and ensemble classifier," *Neural Computing and Applications*, vol. 34, no. 12, pp. 9579–9592, Jun. 2022, https://doi.org/10.1007/s00521-020-04842-6.

[19] Y. Han *et al.*, "Histologic subtype classification of non-small cell lung cancer using PET/CT images," *European Journal of Nuclear Medicine and Molecular Imaging*, vol. 48, no. 2, pp. 350–360, Feb. 2021, https://doi.org/10.1007/s00259-020-04771-5.

[20] M. A. Heuvelmans *et al.*, "Screening for Early Lung Cancer, Chronic Obstructive Pulmonary Disease, and Cardiovascular Disease (the Big-3) Using Low-dose Chest Computed Tomography: Current Evidence and Technical Considerations," *Journal of Thoracic Imaging*, vol. 34, no. 3, May 2019, Art. no. 160, https://doi.org/10.1097/RTI.0000000000000379.

[21] K. E. Lowe *et al.*, "COPDGene® 2019: Redefining the Diagnosis of Chronic Obstructive Pulmonary Disease," *Chronic Obstructive Pulmonary Diseases: Journal of the COPD Foundation*, vol. 6, no. 5, pp. 384–399, https://doi.org/10.15326/jcopdf.6.5.2019.0149.

[22] F. Kanavati *et al.*, "A deep learning model for the classification of indeterminate lung carcinoma in biopsy whole slide images," *Scientific Reports*, vol. 11, no. 1, Apr. 2021, Art. no. 8110, https://doi.org/10.1038/s41598-021-87644-7.

[23] S. Albahli and G. N. Ahmad Hassan Yar, "AI-driven deep convolutional neural networks for chest X-ray pathology identification," *Journal of X-Ray Science and Technology*, vol. 30, no. 2, pp. 365–376, Mar. 2022, https://doi.org/10.3233/XST-211082.

[24] S. Mahima, S. Kezia, and E. Grace Mary Kanaga, "Deep Learning-Based Lung Cancer Detection," in *Disruptive Technologies for Big Data and Cloud Applications*, 2022, pp. 633–641, https://doi.org/10.1007/978-981-19-2177-3_59.

[25] Y. Xu *et al.*, "Deep Learning Predicts Lung Cancer Treatment Response from Serial Medical Imaging," *Clinical Cancer Research*, vol. 25, no. 11, pp. 3266–3275, Jun. 2019, https://doi.org/10.1158/1078-0432.CCR-18-2495.

[26] M. A. Talukder, "Lung X-Ray Image." Mendeley Data, Oct. 24, 2023, https://doi.org/10.17632/9D55CTTN5H.1.

[27] R. H. Abiyev and M. K. S. Ma'aitah, "Deep Convolutional Neural Networks for Chest Diseases Detection," *Journal of Healthcare Engineering*, vol. 2018, pp. 1–11, Aug. 2018, https://doi.org/10.1155/2018/4168538.

[28] R. Tandon, S. Agrawal, A. Chang, and S. S. Band, "VCNet: Hybrid Deep Learning Model for Detection and Classification of Lung Carcinoma Using Chest Radiographs," *Frontiers in Public Health*, vol. 10, Jun. 2022, https://doi.org/10.3389/fpubh.2022.894920.

[29] A. Ait Nasser and M. A. Akhloufi, "A Review of Recent Advances in Deep Learning Models for Chest Disease Detection Using Radiography," *Diagnostics*, vol. 13, no. 1, Jan. 2023, Art. no. 159, https://doi.org/10.3390/diagnostics13010159.